IOSR Journal of Mechanical and Civil Engineering (IOSR-JMCE)
e-ISSN: 2278-1684,p-ISSN: 2320-334X, Volume 13, Issue 1 Ver. IV(Jan. - Feb. 2016), PP 101-108
www.iosrjournals.org

Thermodynamic analysis of LiBr and water based vapour absorption air-conditioning system utilizing waste exhaust heat energy of Diesel Engine

Shakti Prakash Jena*, Smrutirekha Mishra
Department of Mechanical Engineering, SOA University, Bhubaneswar, Odisha, India
***Corresponding Author:** SHAKTI PRAKASH JENA, SOA University, Bhubaneswar, India

Abstract: *The potential of an engine exhaust driven LiBr-water based absorption system for air-conditioning is analyzed in this paper. The effects of generator, condenser, evaporator, and absorber temperatures on the energy and exergy performance of the absorption system were observed. The results indicate that the coefficient of performance increases with increase in evaporator temperature, but decreases with increase in condenser and absorber temperature. The exergy analysis of the system indicates that air cooled condenser and absorber shows higher exergy losses than the generator and evaporator. A small scale LiBr-water based absorption system can be feasible to operate using exhaust heat energy from a diesel engine.*

Keywords- *Absorption Refrigeration, Diesel Engine, Energy, Exergy Efficiency, Exergy losses*

I. Introduction

In recent years, global warming and ozone depletion have stimulated the researchers to focus their interest in absorption based cooling systems. These systems utilize such absorbent and refrigerant pairs, which have very low or negligible ozone depleting effect. On the other hand absorption based cooling system can be operated using waste heat energy as input. Hence industrial waste heat and heat energy from engine exhaust can be utilized to operate such system. As a result it will reduce the thermal pollution to control global warming with production of cooling effect in an eco friendly way [1, 2]. However it's COP is comparatively low from that of vapour compression refrigeration system (VCRS).

This limitation can be over looked, as vapour absorption systems (VAS) are operated on low grade thermal energies and most importantly it allows avoiding use of chlorofluorocarbons (CFCs) that possess high degree of ozone depletion and a major source of electricity consumer, which causes high demand of electricity during peak summer [3]. It is crucial to promote absorption based cooling system to meet the cooling demand in place of VCRS. A number of researchers have investigated the performance a VAS with aqua-ammonia and lithium bromide (LiBr) – water as absorbent refrigerant pair, with cooling capacity ranges from 5 to 50 kW [4]. Small scale cooling system gives very low COP with slow cooling rate, which require a focus for improvement of its COP with compact designing. Additionally the small scale system must be operating on low temperature driving source. Most of the researchers inclined their work towards aqua-ammonia pair because of the low boiling temperature of ammonia (-33˚ C), which allows to go for cooling effect below 0˚ C [5, 6]. Ammonia is corrosive to copper tubings, toxic and flammable in nature. In addition to these limitations, water as absorbent is reasonably volatile which leads to presence of appreciable amount of water vapour in ammonia vapour leaving the generator. This may result in clogging of evaporator tubing due to which an analyser and a rectifier is used in aqua-ammonia system, which increases the system complexity [7]. Based on these restrictions of aqua-ammonia system, LiBr-water absorption system based air-conditioning will be more suitable for study. In this respect, improvement of performance of a LiBr-water absorption cycle using exhaust heat energy from a diesel engine has been investigated in this paper. The thermodynamic analysis of a model LiBr-water absorption cycle with 3.5 kW cooling load is performed to locate the components of the system where exergy losses are affecting the thermal performance of the system.

II. Cycle Operation Principles

A LiBr-water based absorption system linked to a 10 KW diesel engine, to utilize the exhaust heat energy of the engine to heat the solution in the generator. The schematic diagram of the engine exhaust operated LiBr-water absorption cooling system is shown in Fig 1. The weak LiBr solution is heated in the generator by the exhaust heat and water evaporates, leaving strong solution of LiBr in the generator. The evaporated water vapour at high pressure (State 1) enters to the condenser, where it is condensed to high pressure liquid water (State 2). Then the liquid water is expanded to the evaporator pressure through a throttle valve (State 3) and flows through the evaporator results in cooling effect of the desired space, and then the vapour of water from the evaporator enters to the absorber (State 4). The strong solution of LiBr coming from the generator through

solution heat exchanger is expanded to the absorber pressure by another throttle valve (State 8 -10), absorbs the refrigerant vapour coming from evaporator, and becomes a weak solution in the absorber releasing heat of absorption. Again the weak solution from the absorber is pumped to the generator by a solution pump through the solution heat exchanger (State 5-7). The solution heat exchanger attached in between generator and absorber to improve the performance of the system. In VAS the pump is the only part which requires work input. This work input is comparatively very small than that of the work input required by a compressor of a VCRS [8]. Due to the high vaporisation heat of water as compared to ammonia, LiBr-water cycle leads to a higher COP than that of ammonia- water at same cooling capacity [9]. The heat flow pattern of the LiBr-water absorption cycle is depicted in Fig 2. The energy and exergy analysis is getting more attention at present to evaluate the performance of a thermal energy system. The maximum potential for a system to perform work is a function of its internal energy and the ambient conditions. The system energy balance deals with energy distribution based on system integration [10, 11]. Focusing on exergy destruction at each components, the energy and exergy analysis were performed to improve the performance of the vapour absorption based cooling system.

III. Thermodynamic model

The thermodynamic analysis of the VAS is done based on principle of mass conservation, energy conservation, and second law of thermodynamics and applied to analyze each components of the system.

3.1 Energy and Exergy analysis

In this investigation the following principal equations are used to determine the mass and energy conservation at each component. For the generator, the mass and energy balances are:

Total mass balance: $\dot{m}_7 = \dot{m}_1 + \dot{m}_8$ (1)

LiBr mass balance: $X_7 \dot{m}_7 = X_8 \dot{m}_8$ (2)

Where, $\dot{m}$ is the mass flow rate (Kg/s) and X_7 and X_8 are the mass fraction of LiBr in solution at respective states.

Heat transfer rate for generator $\dot{Q}_g$ is calculated as:

$$\dot{Q}_g = \dot{m}_1 h_1 + \dot{m}_8 h_8 - \dot{m}_7 h_7 \quad (3)$$

Where, h is the specific enthalpy (kJ/Kg). The mass flow rate of weak and strong solutions can be calculated from equations (4) and (5) respectively.

$$\dot{m}_7 = \frac{\dot{m}_1 X_8}{X_8 - X_7} \quad (4)$$

$$\dot{m}_8 = \frac{\dot{m}_1 X_7}{X_8 - X_7} \quad (5)$$

Energy balance for the solution heat exchanger is calculated by equation (6) and (7).

$$T_9 = \varepsilon T_6 + (1 - \varepsilon) T_8 \quad (6)$$

Where, ε = 80%, is effectiveness of the solution heat exchanger.

$$h_7 = h_6 + \frac{\dot{m}_8}{\dot{m}_6}(h_8 - h_9) \quad (7)$$

The energy increase by pumping is calculated as:

$$h_6 = h_5 + \frac{\dot{W}_p}{\dot{m}_6} \quad (8)$$

$$\dot{W}_p = \dot{m}_6 (P_6 - P_5) v_6 \quad (9)$$

Where, $\dot{W}_p$ is Pump Work.

Energy balance for the condenser, evaporator and absorber are calculated as:

$$\dot{Q}_{con} = \dot{m}_1 (h_1 - h_2) \quad (10)$$

$$\dot{Q}_{eva} = \dot{m}_1 (h_4 - h_3) \quad (11)$$

$$\dot{Q}_{ab} = \dot{m}_4 h_4 + \dot{m}_{10} h_{10} - \dot{m}_5 h_5 \quad (12)$$

$$COP = \frac{\dot{Q}_{eva}}{\dot{Q}_g + \dot{W}_p} \quad (13)$$

Exergy analysis overcomes the restrictions of the first law of thermodynamics and is based on both the first and second laws of thermodynamics. By optimizing the energy distribution of all the systems, losses can be minimized. In this study the chemical exergy is neglected [12, 13], so the exergy per unit mass can be defined as [14]:

$$e = (h - h_0) - T_0(s - s_0) \quad (14)$$

Where, 'e' is the specific exergy, 'h' and's' are the enthalpy and entropy respectively of the fluid at temperature 'T', whereas, 'h_0' and 's_0' and's' are the enthalpy and entropy respectively of the fluid at environmental temperature T_0 (303 K). The exergy loss in each component and the total exergy loss for the system can be calculated as:

$$\dot{E}_{D,g} = \dot{m}_7 e_7 - \dot{m}_8 e_8 - \dot{m}_1 e_1 + \dot{Q}_g \left(1 - \frac{T_0}{T_g}\right) \quad (15)$$

$$\dot{E}_{D,con} = \dot{m}_1 (e_1 - e_2) - \dot{Q}_{con} \left(1 - \frac{T_0}{T_{con}}\right) \quad (16)$$

$$\dot{E}_{D,eva} = \dot{m}_1 (e_3 - e_4) + \dot{Q}_{eva} \left(1 - \frac{T_0}{T_{eva}}\right) \quad (17)$$

$$\dot{E}_{D,ab} = \dot{m}_4 e_4 + \dot{m}_{10} e_{10} - \dot{m}_5 e_5 - \dot{Q}_{ab} \left(1 - \frac{T_0}{T_{ab}}\right) \quad (18)$$

$$\dot{E}_{D,Total} = \dot{E}_{D,g} + \dot{E}_{D,con} + \dot{E}_{D,eva} + \dot{E}_{D,ab} \quad (19)$$

Where, '$\dot{E}_D$' is the specific rate of exergy losses or exergy destruction. The ideal thermal performance of a VAS is determined by assuming that the entire cycle is reversible in nature [8], in that case the reversible COP can be calculated as:

$$\text{Re versible} \quad COP = \left(1 - \frac{T_0}{T_g}\right)\left(\frac{T_{eva}}{T_0 - T_{eva}}\right) \quad (20)$$

IV. Thermodynamic Properties

In the schematic diagram state (1) to (4) requires the thermodynamic properties of water and state (5) to (10) are based on LiBr- water mixture. The specific enthalpy and entropy of the LiBr- water mixture is calculated by using correlations from reference [15]. The following assumptions were considered during the study:

- The system is operated under steady state conditions.
- Pressure drops and heat transfer losses in the pipelines are neglected.
- Expansion of the LiBr- water mixture through throttle valves is isenthalpic in nature.
- The solution pump is isentropic in nature.
- The refrigerant states at outlet of condenser and evaporator are saturated liquid and saturated vapour respectively.

V. Results and discussion

The performance of each component of the LiBr-water based VAS are analyzed and discussed in this section. The COP and reversible COP are represented graphically with variation of temperature for each component. Heat transfer between two finite temperature, mixing losses and pumping losses leads the system to irreversibility [16, 17].

5.1. Effects of variation in generator temperature with cop and exergy of air-conditioning system

The variation of COP and reversible COP with generator temperature is shown in Fig. 3. The reversible COP increases with increase in generator temperature, while COP decreases with increase in temperature beyond 80° C. This may be due to increase in finite temperature difference between heat-exchange, which also affects the exergy efficiency of the system. Although the higher generator temperature will produce more

refrigerant vapour, at the same time it will lead to increase in temperature of the solution in the absorber. This will result in increase in absorber load and will affect the absorption process leading to increase in mixing losses; as a result reduces the COP and exergy efficiency with an increase in total exergy losses. Fig 4. shows the variation of exergy efficiency and total exergy loss with generator temperature. With increase in generator temperature up to 110˚ C the exergy efficiency reduced from 38.66% to 13.98%, and total exergy loss increased from 0.372 to 0.603 kW.

5.2. Effects of variation in evaporator temperature with cop and exergy of air-conditioning system

Fig 5. represents the variation of COP and reversible COP with evaporator temperature. Increase in evaporator temperature increases the vapour pressure in the absorber, leads in significant increase in absorption process of the strong solution. At constant cooling load with increase in evaporator temperature, generator load and absorber load also decreases [17]. The result also illustrates that the increase in COP with evaporator temperature is quite linear as in comparison to that of increase in reversible COP. This leads to decrease in exergy efficiency of the system with increase in evaporator temperature. The variation of exergy efficiency and total exergy loss with evaporator temperature is shown in Figure 6. The curve indicates an increase in total exergy loss. With increase in evaporator temperature from 6˚ C to 14˚ C the exergy efficiency reduced from 37.97% to 25.5%, and total exergy loss increased from 0.343 to 0.612 kW. This can be concluded that, the desired cooling effect can be reached by decreasing the evaporator temperature, which should be limited to 6˚ C as corresponding saturation pressure would be very low for water as refrigerant.

5.3. Effects of variation in condenser temperature with COP and exergy of air-conditioning system

The variation of COP and reversible COP with condenser temperature is presented in Fig 7. Condenser temperature does not have any impact on reversible COP, while a slight decrease in COP is observed. The coefficient of performance of a vapour absorption cycle under reversible condition depends on heat supplied from the source (generator temperature) and heat removed from the air-conditioned space by the evaporator (evaporator temperature). Hence reversible COP remains unaffected by variation of condenser temperature. If cooling load is kept constant then with increase in condenser temperature, corresponding condensation pressure increases. This leads in increase in load on the generator, as a result the COP decreases. It is also observed from Fig 8. that, the exergy efficiency slightly decreases with increase in condenser temperature, while the total exergy loss also increases rapidly with increasing condenser temperature. This can be related to increase in temperature difference between the condenser refrigerant and environment. With increase in condenser temperature, generator pressure increases leading to increase in generator load and absorber load. As a result exergy losses increases in condenser and absorber; leading to decrease in exergy efficiency of the system. With increase in condenser temperature up to 60˚ C the exergy efficiency reduced from 38.07% to 31.33%, and total exergy loss increased from 0.322 to 0.973 KW.

5.4. Effects of variation in absorber temperature with COP and exergy of air-conditioning system

Fig 9. represents the variation of COP and reversible COP with absorber temperature, which shows a similar trend as that of the condenser temperature. The absorption efficiency of the strong solution decreases with increase in absorption temperature. This results in increase in generator load and absorber load with increase in mixing losses in the absorber. The variation of exergy efficiency and total exergy loss with evaporator temperature is shown in Figure 10. As the temperature difference between the strong solution and weak solution decreases with increase in absorber temperature, negatively impacting the absorption process. This results in major increase in total exergy loss of the system, leading to decrease in exergy efficiency. With increase in absorber temperature up to 50˚ C the exergy efficiency reduced from 45.51% to 19.56%, and total exergy loss increased from 0.144 to 0.786 kW.

VI. Conclusions

The main aim of this investigation was to analyze the performance of a LiBr-water absorption cycle using exhaust heat energy from a diesel engine.

1. The results indicate that the COP decreases with increase in generator, condenser and absorber temperature and insignificant with increase in evaporator temperature. With variation in operating conditions the COP of the system ranges from 0.42 to 0.76, whereas reversible COP varies from 1.65 to 2.95.
2. The exergy analysis of the system indicates that air cooled condenser and absorber shows higher exergy losses than the generator and evaporator. The analysis reveals that, by maintaining the condenser temperature and absorber temperature close to ambient temperature will not affect significantly the performance of the absorption cycle.

3. This will require an optimised design of the condenser and absorber for small scale application of LiBr-water base absorption cooling system. The small scale LiBr-water base absorption cooling system can be feasible to operate with exhaust energy from a diesel engine.

References

[1] S Aphornratana. , I.W Eames, Thermodynamic analysis of absorption refrigeration cycles using the second law of thermodynamics method, *International Journal of Refrigeration, 18, 244-252, 1995*.

[2] M.I. Karamangil, S. Coskun, O. Kayankli, , N. Yamankaradeniz, 2010. A simulation study of performance evaluation of single-stage absorption refrigeration system using conventional working fluids and alternatives. *Renew Sustain Energy Rev. 14, 1969-78.*

[3] L. Trygg, , S. Amiri, , 2007. European perspective on absorption cooling in a combined heat and power system- a case study of energy utility and industries in Sweden. *Applied Energy. 84, 1319-37.*

[4] H.Z Hassan, A.A Mohamad, 2012. A review on solar cold production through absorption technology. *Renewable and Sustainable Energy Reviews. 16, 5331–5348*.

[5] F. Boudenenn, H.. Demasles, J. Wyttenbach, X. Jobard, D. Cheze, P. Papillon, 2012. Development of a 5 kW cooling capacity ammonia-water absorption chiller for solar cooling applications. *Energy Procedia. 30, 35-43*.

[6] J.M. Abdulateef, K. Sopi, M.A. Alghoul, 2008. Optimum design for solar absorption refrigeration systems and comparison of the performances using ammonia-water, ammonia-lithium nitrate and ammonium- sodium thiocyanate solutions. *International Journal Mechanical Master Engineering. 3, 17-24.*

[7] I. Horuz, 1998. A comparison between ammonia-water and water –lithium bromide solutions in vapour absorption refrigeration systems. *Int. Comm. Heat Mass Transfer. 25, (5), 711-721.*

[8] Y. Cengel, M. Boles, 2008. *Thermodynamics: An Engineering Approach ,fifth ed. McGra-Hill.*

[9] R. Gomri, 2010. Investigation of the potential of application of single effect and multiple effect absorption cooling systems. *Energy Convers. Manage. 51, 1629-1636*.

[10] S.P. Jena, S.K. Acharya, C. Deheri, 2015. Thermodynamic analysis of a twin cylinder diesel engine in dual fuel mode with producer gas. *Biofuels, doi.org/10.1080/17597269.2015.1118779*.

[11] G.Q Chen, 2005. Exergy consumption of the earth Ecological Modelling *184: 363-380*.

[12] C.D. Rakopoulos, E.G. Giakoumis 2006. Second law analyses applied to internal combustion engine operation. *Progress in Energy and Combustion Science 32 (1): 2–47.*

[13] R. Vidal, R. Best, R. Rivero, J. Cerventas, 2006. Analysis of a combined power and refrigeration cycle by the exergy method. *Energy 31, 3401-3414.*

[14] L. Zhu, J. Gu 2010. Second law-based thermodynamic analysis of ammonia/sodium thiocyanate absorption system. *Renewable Energy 35, 1940-1946.*

[15] H.T. Chua, H.K. Toh, A. Malek, K.C. Ng, K. Srinivasan 2000. Improved thermodynamic property fields of LiBr-H2O solution. *International Journal of Refrigeration 23, 412-429.*

[16] J. Aman, D.S.K. Ting, P. Henshaw 2014. Residential solar air conditioning: Energyand exergy analyses of an ammonia-water absorption cooling system. *Applied Thermal Engineering 62, 424-432*.

[17] S.C. Kaushik, A. Arora 2009. Energy and exergy analysis of single effect and series flow double effect water-lithium bromide absorption refrigeration systems. *International Journal of Refrigeration 32, 1247-1258*.

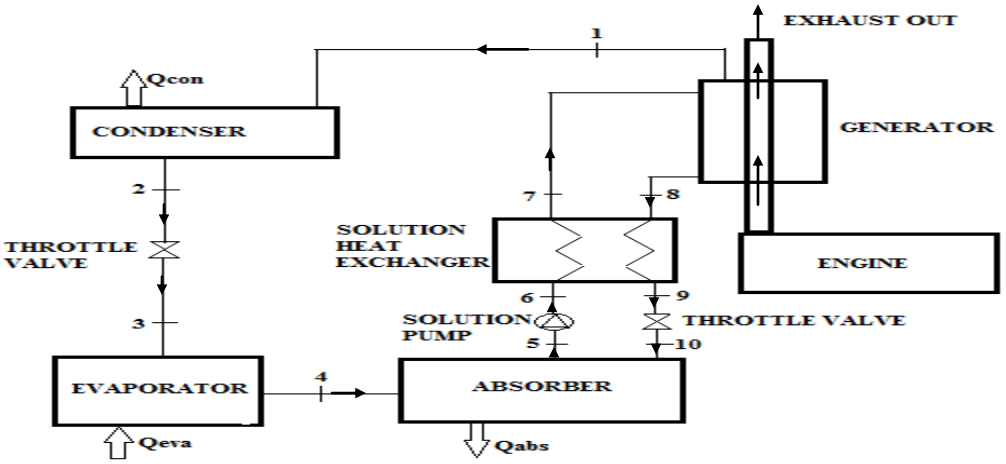

Fig. 1 Schematic diagram of the exhaust energy based LiBr-water absorption system.

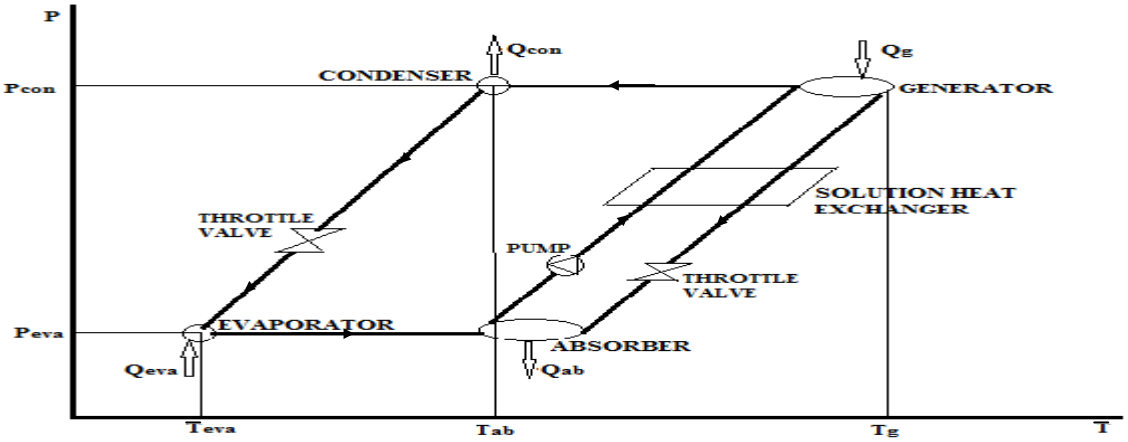

Fig. 2 Temperature, pressure and concentration diagram of LiBr-water mixture [4].

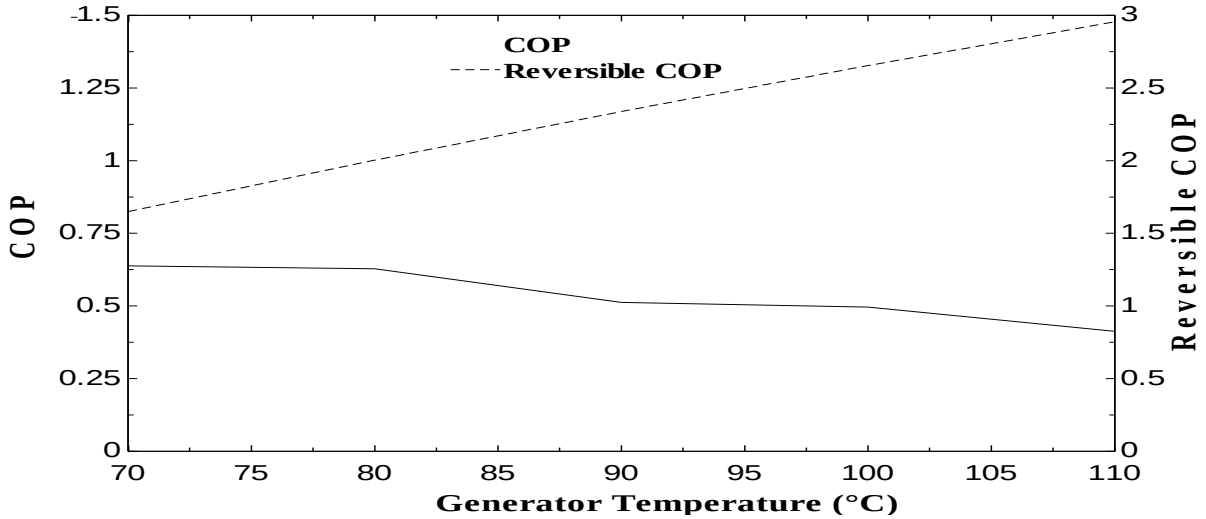

Fig. 3 Variation of COP and reversible COP with generator temperature at T_{con}= 40˚C, T_{ab}= 40˚C, T_{eva}= 10˚C.

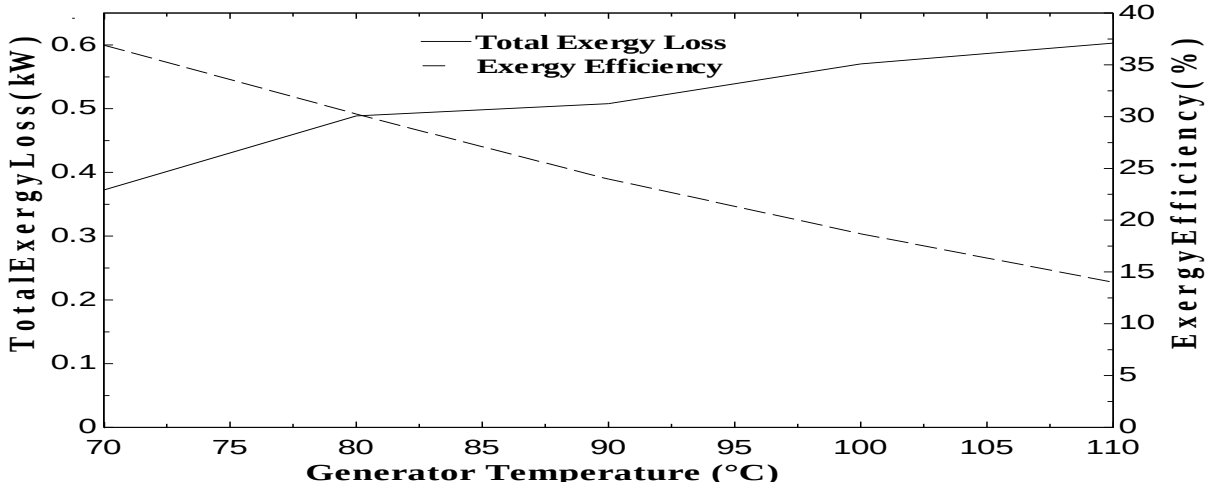

Fig. 4 Effect of generator temperature on total exergy loss and exergy efficiency at T_{con}= 40˚C, T_{ab}= 40˚C, T_{eva}= 10˚C.

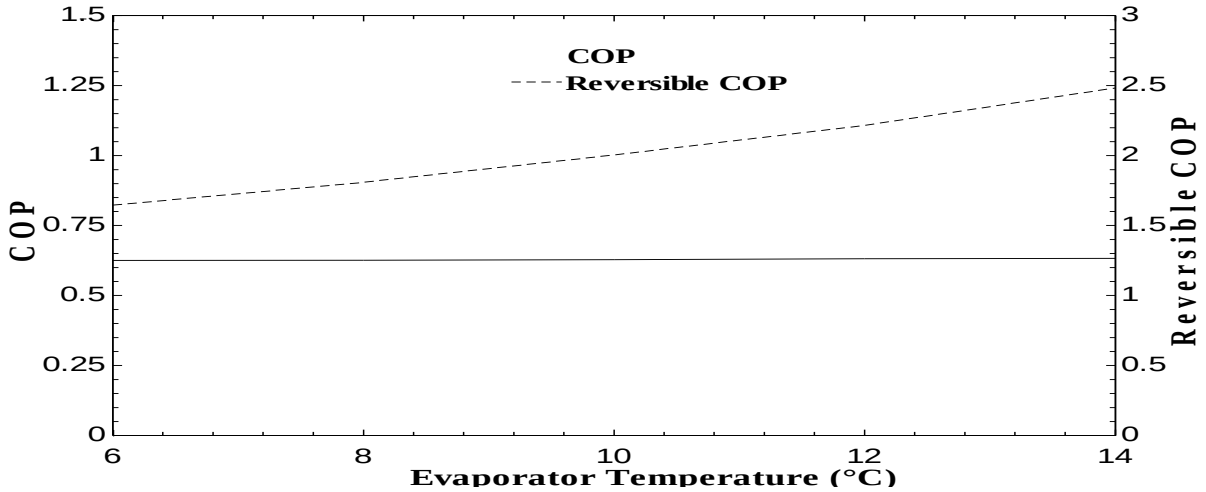

Fig. 5 Variation of COP and reversible COP with evaporator temperature at T_{con}= 40˚C, T_{ab}= 40˚C, T_g= 80˚C.

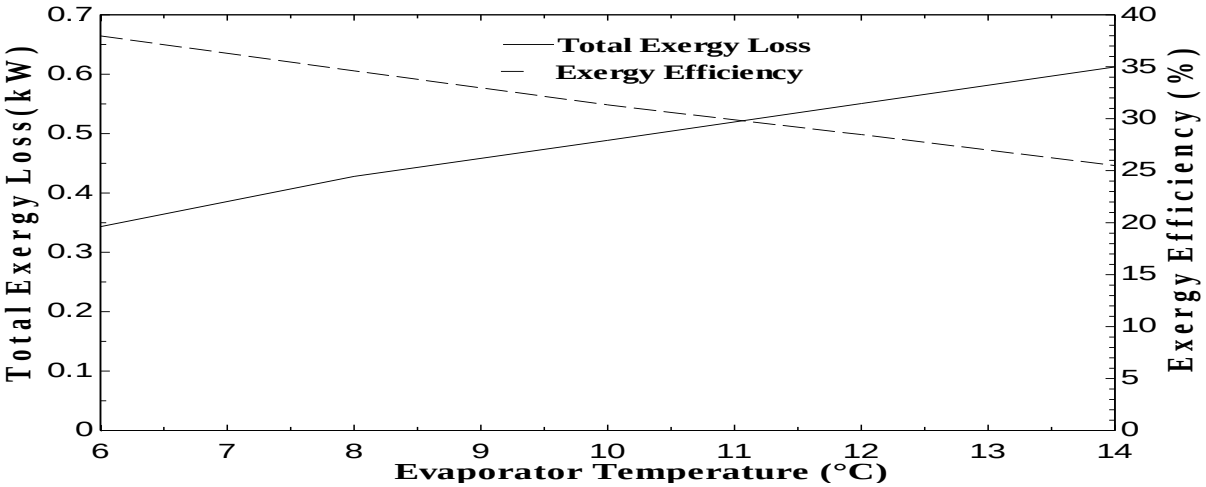

Fig. 6 Effect of evaporator temperature on total exergy loss and exergy efficiency at T_{con}= 40˚C, T_{ab}= 40˚C, T_g= 80˚C.

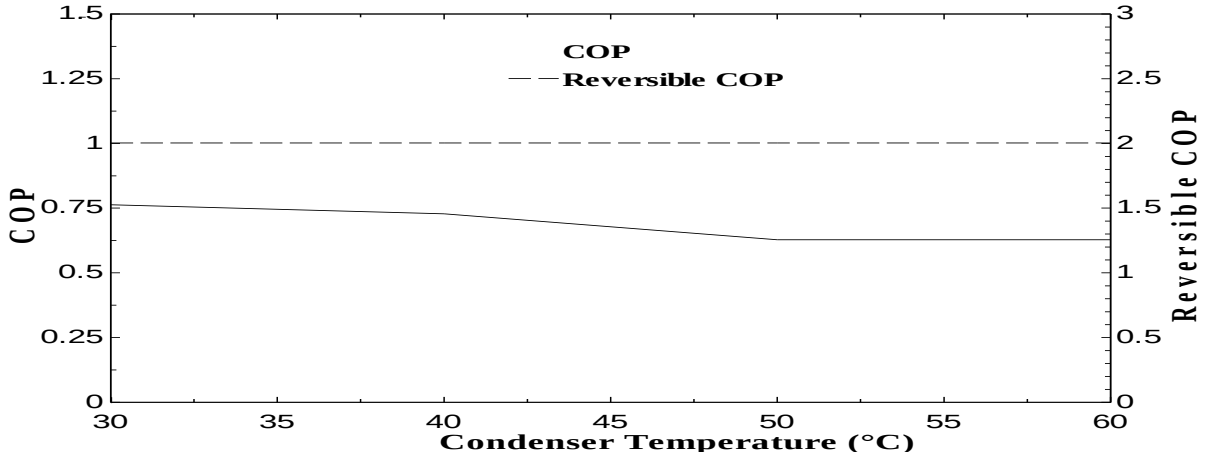

Fig. 7 Variation of COP and reversible COP with condenser temperature at T_g= 80˚C, T_{ab}= 40˚C, T_{eva}= 10˚C.

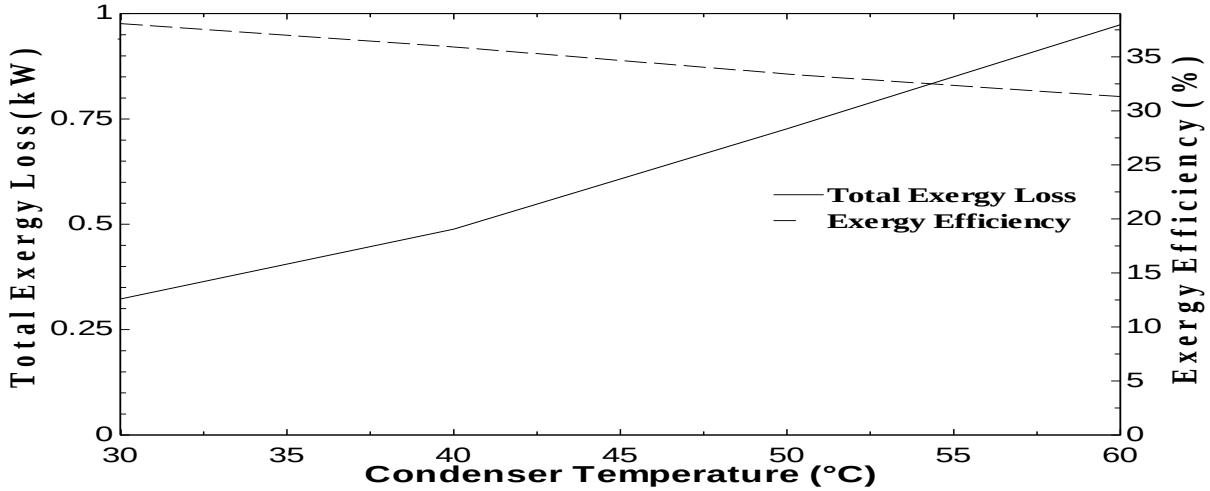

Fig. 8 Effect of condenser temperature on total exergy loss and exergy efficiency at T_g= 80˚C, T_{ab}= 40˚C, T_{eva}= 10˚C.

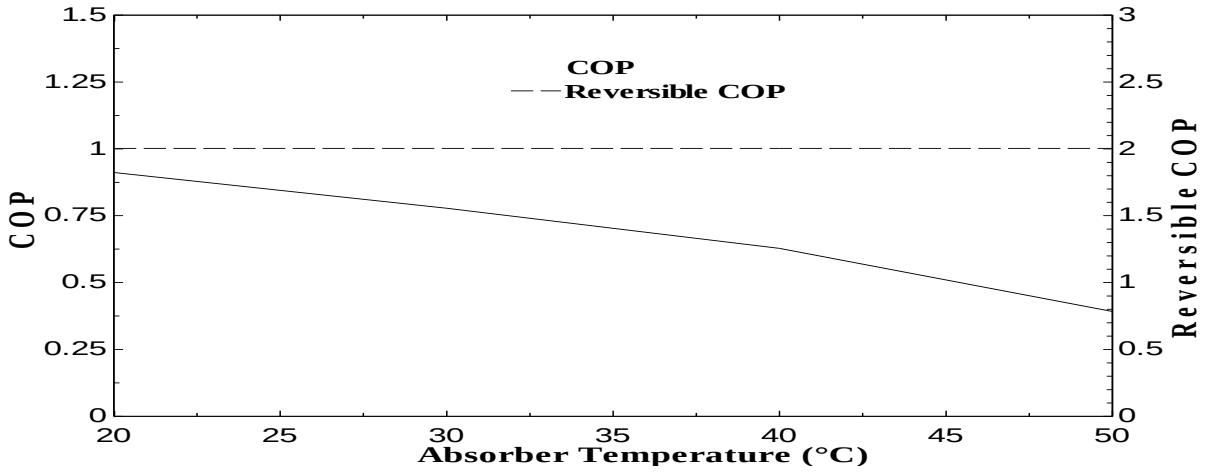

Fig. 9 Variation of COP and reversible COP with absorber temperature at T_g= 80˚C, T_{con}= 40˚C, T_{eva}= 10˚C.

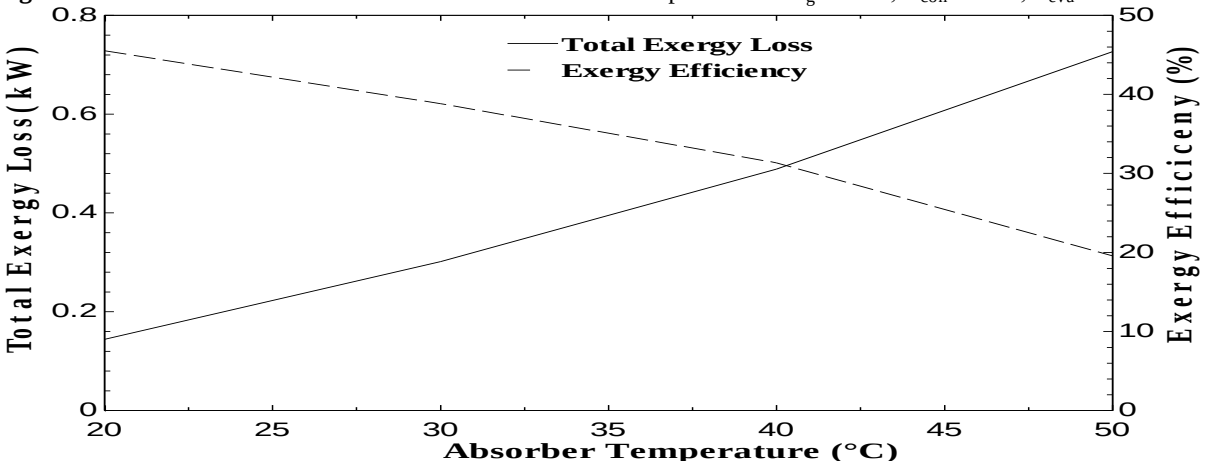

Fig. 10 Effect of absorber temperature on total exergy loss and exergy efficiency at T_g= 80˚C, T_{con}= 40˚C, T_{eva}= 10˚C.